Plane-wave X-ray topography and its application at SPring-8

Satoshi Iida,[a]* Yoshinori Chikaura,[b] Seiji Kawado[c] and Shigeru Kimura[d]

[a]Department of Physics, Toyama University, Toyama 930-8555, Japan, [b]Faculty of Engineering, Kyushu Institute of Technology, Kitakyushu-shi 804-8550, Japan, [c]Rigaku Corporation, Akishima, Tokyo 196-8666, Japan, and [d]Fundamental Research Laboratories, NEC Corporation, Tsukuba, Ibaraki 305-8501, Japan. E-mail: sxiida@sci.toyama-u.ac.jp

Plane-wave X-ray topography experiments were carried out at a 200 m-long beamline, BL20B2, at SPring-8. Relatively high-energy X-rays of 30 keV with an angular divergence of about 0.01 arcsec were produced by using only one collimator crystal. FZ-Si and CZ-Si wafers were characterized in transmission geometry (Laue case). Clear oscillatory profiles in rocking curves of the FZ-Si crystal were observed. Plane-wave topographic images of dislocations, growth striations and grown-in microdefects in the CZ-Si crystals were obtained. The dependence of the topographic images of the lattice defects on the sample–photoplate distance was also studied.

Keywords: X-ray topography; plane-wave; silicon crystal; lattice defects.

1. Introduction

Plane-wave X-ray topography is an X-ray diffraction imaging technique in which highly collimated X-rays with an angular divergence much less than the Darwin width of the Bragg reflection are used. Ishikawa (1989) developed plane-wave topography using intense and brilliant synchrotron radiation and stable precision goniometers at the Photon Factory, KEK, Japan. After demonstration of the high sensitivity of plane-wave topography to lattice strain by Ishikawa (1989), plane-wave topography has been extensively applied to evaluation of minute lattice strains in silicon crystals. Although the silicon crystals are dislocation-free, grown-in and process-induced defects are observed in silicon crystal wafers. Characterization and control of these defects are important issues for present silicon crystal technology. However, these defects would hardly be detected by using conventional topography. Kawado *et al.* (1990) and Kudo *et al.* (1997) applied plane-wave topography to the quantitative analysis of growth striations in magnetic-field-applied Czochralski silicon (CZ-Si) single crystals. Kimura *et al.* (1992, 1994, 1996) characterized the A- and D-defects in float-zone-grown silicon (FZ-Si) crystals using plane-wave topography combined with oscillatory profile measurement of the rocking curves in the Laue case (transmission geometry). Chikaura *et al.* (1990) and Suzuki *et al.* (1993) showed that plane-wave topography was effective for thinned crystals with thicknesses of the order of the extinction distance and was sensitive for imaging microdefects in as-grown CZ-Si and annealed CZ-Si crystals.

In this paper, the production of a highly parallel X-ray beam and the development of plane-wave topography at the beamline (BL) 20B2 of SPring-8 are described. BL20B2 is a medium-length beamline at SPring-8 and is allocated to X-ray imaging and medical applications (Goto *et al.*, 2001). At a second experimental station of BL20B2, a high-precision diffractometer for a multiple-crystal arrangement was constructed (Chikaura *et al.*, 2001). At this station, highly collimated X-rays can be produced by only one collimator crystal. Simple optics to produce the highly collimated X-rays at BL20B2 allow us to carry out plane-wave topography experiments easily. We can also use relatively high-energy X-rays for plane-wave topography at SPring-8, which is another favourable point because we can characterize Si wafers of usual thickness. Characterization of three silicon crystals, *i.e.* highly perfect FZ-Si, CZ-Si containing dislocations and CZ-Si containing grown-in microdefects, has been carried out. The dependence of the defect images on the sample–photoplate distance has been studied.

2. Experimental

Fig. 1 shows our experimental set-up for plane-wave topography. Synchrotron radiation from a bending-magnet source was monochromated to 30 keV (0.4 Å) by the standard double-crystal monochromator using the 311 reflection in the optics hutch 36.8 m from the source point. The angular divergence of the monochromated X-rays was further lowered by a collimator crystal in the second experimental hutch located at 200 m from the source point. The collimator crystal was made from a ⟨110⟩-grown FZ-Si, 3" in diameter and 10 mm thick. The X-ray incidence surface of the collimator crystal, cut 6° from the crystal growth axis, was mechanochemically mirror polished. An asymmetric 220 reflection was used with an incident angle of about 0.2°. The resulting asymmetric factor was about 1/60.

Three sample crystals were examined by plane-wave topography. The first crystal was a (111) FZ-Si wafer of thickness 0.360 mm. The second crystal was a (110) silicon plate cut from ⟨111⟩-grown CZ-Si. This crystal contained dislocations in the necking part. The third was a 0.518 mm-thick (100) plate of as-grown CZ-Si pulled at a rate of 0.4 mm min^{-1}, p-type, 10 Ω cm.

The collimator crystal and the sample crystals were set on a horizontal axis using precision goniometers of the tangential-bar type. Rocking curves of the collimator and the sample crystals were measured using a scintillation counter or an ion-chamber. Topographic images of the sample crystals in the symmetric Laue case were recorded on an imaging plate with a pixel size of 50 μm × 50 μm (Blue IP), or nuclear photoplates, Ilford L4, 25 μm or 50 μm thick.

Topographic images were recorded at three different positions from the sample in order to study change of the topographic images owing to propagation of the diffracted X-rays in free space. The so-called propagation method to observe the angular distribution of the X-rays is much simpler and easier to achieve than the method which needs a sophisticated multi-crystal arrangement using an analyzer crystal (Ishikawa, 1989).

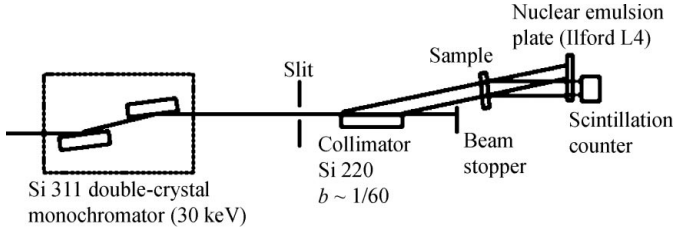

Figure 1
Schematic diagram of the experimental arrangement for plane-wave X-ray diffraction topography. The double-crystal monochromator was placed in the optics hutch, and the collimator and sample crystals were set on precision goniometers installed in the second experimental station.

3. Results and discussion

A rocking curve of the collimator crystal is shown in Fig. 2. The full width at half-maximum (FWHM) of the rocking curve was 9 arcsec, almost equal to the theoretically expected value for a silicon 220 reflection. The FWHM of the 311 reflection from the monochromator was about 0.7 arcsec and angular width accepted by the collimator crystal was about 0.4 arcsec. Therefore, the angular width of the collimated X-rays was estimated to be about 0.01 arcsec based upon the asymmetric factor of the collimator crystal.

Fig. 3(*a*) shows a rocking curve of the FZ-Si wafer, 220 reflection in the symmetric Laue geometry, measured with an aperture of 1 mm × 2 mm in front of the detector. An oscillatory profile was clearly observed as expected from the dynamical theory of X-ray diffraction. Fig. 3(*b*) shows a theoretical rocking curve calculated by the dynamical theory of X-ray diffraction with parameters, $f' = 0.01532$, $f'' = 0.0226$ and a thickness of 0.360 mm. No remarkable broadening of the experimental rocking curve was observed as compared with the theoretical curve. Good agreement between the experimental and the theoretical rocking curves indicates that the angular divergence of X-rays impinging on the sample crystal was estimated to be of the order of 0.01 arcsec. It is worthwhile to mention that the plane wave was produced by using only one collimator crystal. This is possible only when the small source size and the long distance (200 m) between the source and the experimental station are realised. On the other hand, in the case of plane-wave topography at the Photon Factory, KEK, Japan, two asymmetrically cut collimator crystals were used successively to obtain the plane-wave X-rays (Ishikawa, 1989). The plane-wave topography at the BL20B2 thus becomes easier and more stable due to the simple optics. Fig. 4 shows a set of topographs of the FZ-Si wafer recorded on a Blue IP. Topographs of 000 (upper) and 220 (lower) reflections were taken at two angular positions of the rocking curve, $\Delta\theta = -0.35$ arcsec (left) and -0.99 arcsec (right) as indicated by the arrows in Fig. 3(*a*).

Plane-wave topographs of the dislocated CZ-Si crystal were taken at the peak of the 111 reflection rocking curve. Figs. 5(*a*) and 5(*b*) show topographs recorded on nuclear photoplates set at 234 cm and 13 cm from the sample, respectively. Dislocations and growth striations are clearly observed. Fig. 6 shows a Lang topograph of the same area of the sample taken with a 111 reflection using Mo $K\alpha$ radiation. Growth striations can be observed with a higher contrast in the plane-wave topographs than in the Lang topograph. Dislocation images in the plane-wave topographs are also clearer than those in the Lang topograph, and do not blur even at a distance 234 cm from the sample.

Plane-wave topographs of the slowly grown CZ-Si crystal were taken at the peak position of the 220 reflection rocking curve. The topographs in bright field (000 reflection) and those in dark field (220 reflection) were recorded on nuclear photoplates set at 6 mm, 78 mm, 218 cm and 215 cm from the sample. Fig. 7 shows a topograph taken 78 mm from the sample using the 220 reflection. Fringes observed in Fig. 7(*a*) result from the oscillatory profile in the rocking curve, that is, each fringe corresponds to equal inclination parts in the slightly warped sample crystal. Fig. 7(*b*) shows an enlarged part of Fig. 7(*a*), where topographic images of grown-in microdefects are observed as dots. The defect density was estimated to be about 300 cm^{-3}, and the defect image sizes were several tens of micrometres. These values are consistent with the results of a previous work obtained by Lang topography using 60 keV synchrotron radiation (Iida *et al.*, 2000). Six topographic images of the bright and dark fields taken at three positions of the detector are shown in Fig. 8. The sizes of the defect images in the topographs

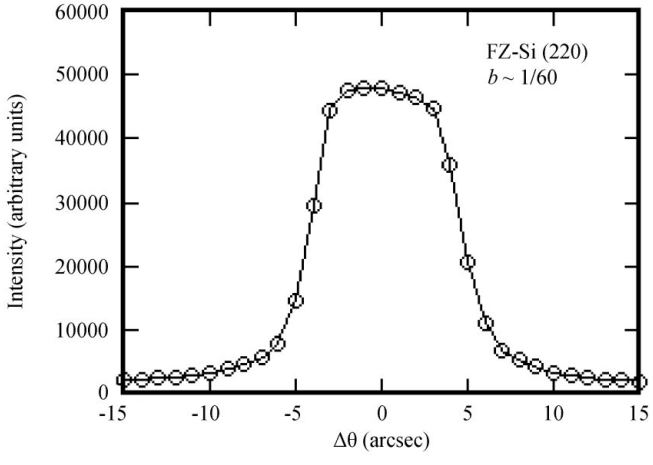

Figure 2
Rocking curve of the collimator crystal. The Si 220 asymmetric reflection at grazing incidence was used.

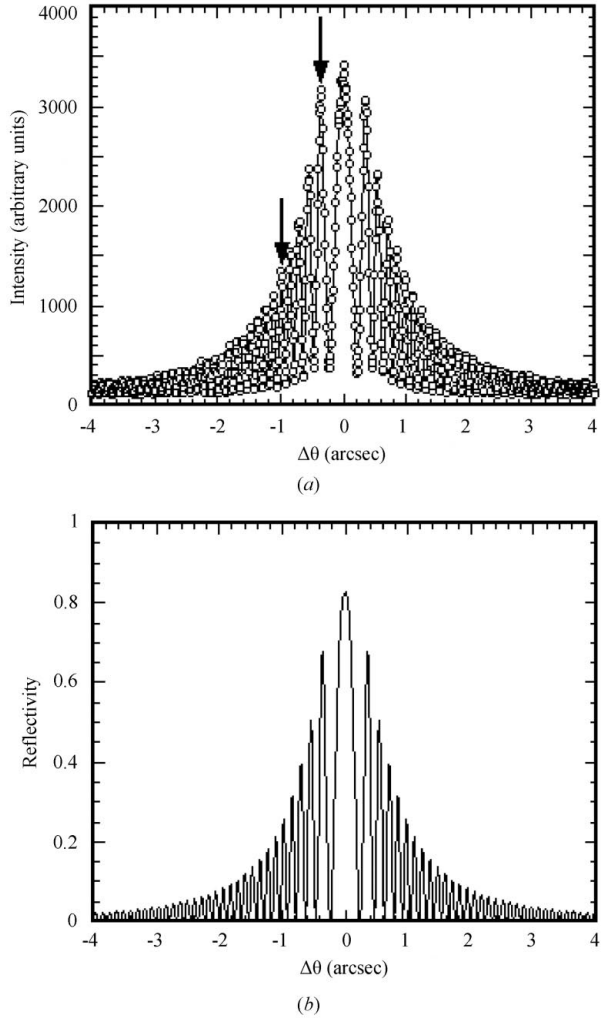

Figure 3
Rocking curves of the FZ-Si wafer, 220 reflection; (*a*) measured and (*b*) calculated for a ideal plane-wave with a crystal thickness of 0.360 mm.

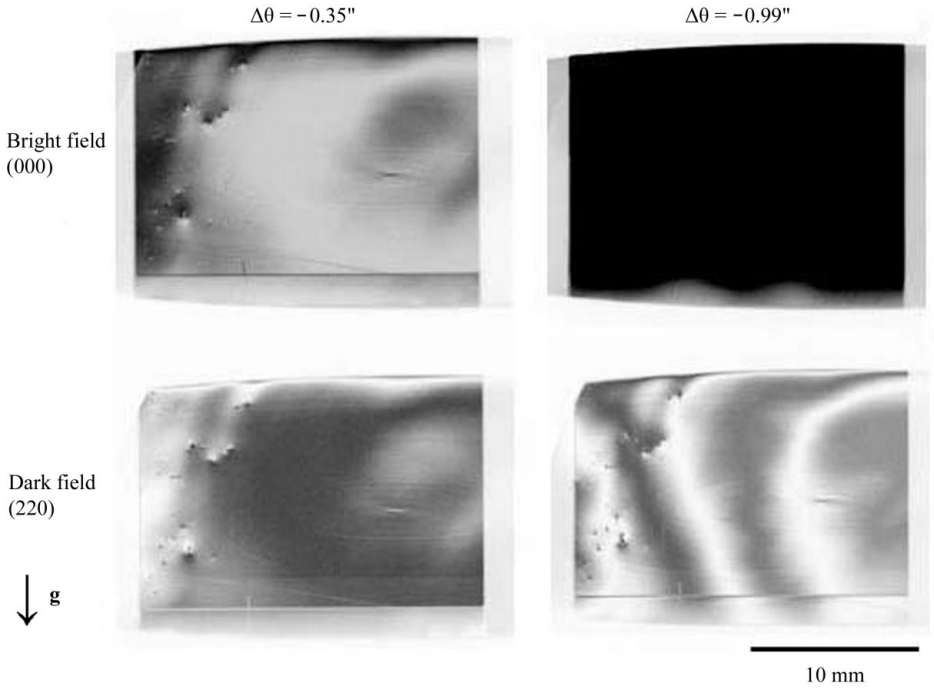

Figure 4
Plane-wave topographs of the FZ-Si wafer, taken with 000 and 220 reflections at $\Delta\theta = -0.35$ and -0.99 arcsec, as indicated by the arrows in Fig. 3(*a*).

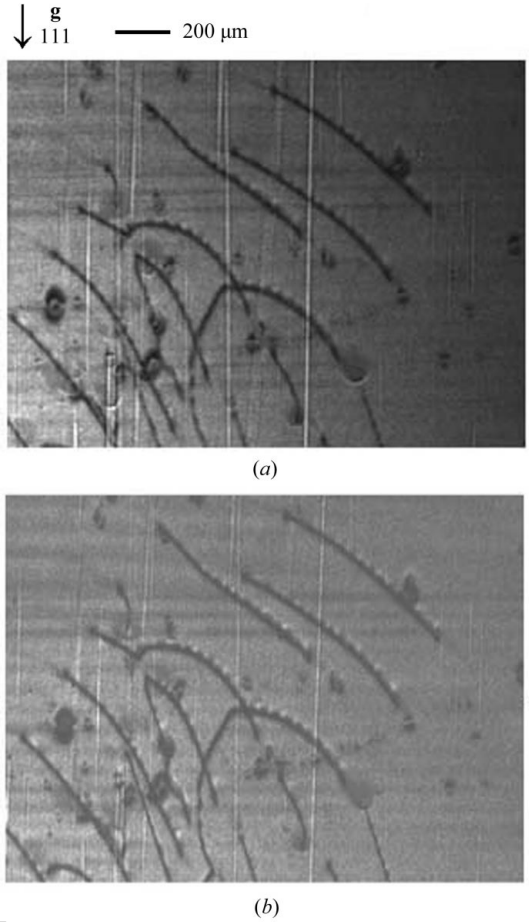

Figure 5
Plane-wave topographs of the CZ-Si wafer containing dislocations, taken at (*a*) 234 cm and (*b*) 13 cm from the sample, using the 111 reflection.

are almost equal to each other. This fact that no remarkable increase in defect image size owing to the wave propagation is observed can be explained as follows. The defect images come from an extended region and are not caused by concentrated strain centres.

The complex black–white contrast of the defect images in Fig. 8 could not be explained by a simple spherical strain field around the defects which was assumed in the analysis of the simple black dot images observed in 60 keV synchrotron radiation Lang topographs (Iida *et al.*, 2000). Transmission electron microscopy (TEM) observations showed that there were interstitial-type dislocation loops or clusters of loops in slowly grown CZ-Si crystals (Takeno *et al.*, 1992; Sadamitsu *et al.*, 1993). The size of the dislocation loops observed by TEM varies from 0.1 to 10 μm between authors. Nango *et al.* (1999) showed that there were large entangled dislocation loops extending over 50–100 μm regions in a slowly pulled CZ-Si crystal by using laser scattering tomography. The lattice defects observed in the plane-wave topographs are probably clusters of dislocation loops or entangled dislocation loops, not a single dislocation loop, because the defect images are complicated. The topographic image contrast changes slightly depending on the sample–film distances. A detailed and quantitative analysis of the microdefect images is in progress and will be reported elsewhere.

4. Conclusions

A plane-wave topography system was constructed at the second experimental station of BL20B2 at SPring-8. Plane-wave X-rays with

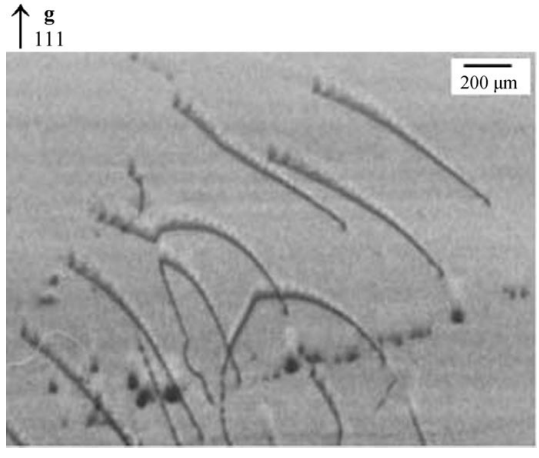

Figure 6
Lang projection topograph of the CZ-Si wafer containing dislocations, taken with the 111 reflection using Mo $K\alpha$ radiation. A part corresponding to that in Fig. 5 is shown.

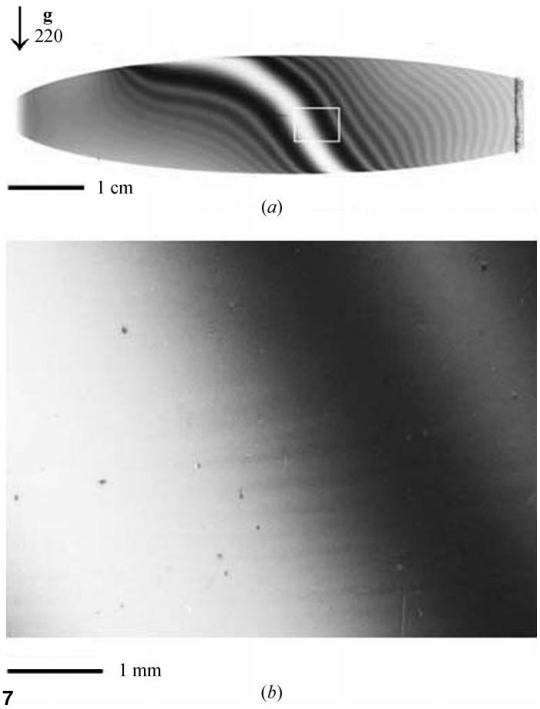

Figure 7
Plane-wave topographs of the slowly grown CZ-Si wafer containing microdefects, taken at 78 mm from the sample using the 220 reflection. The marked area in (*a*) is enlarged and shown in (*b*).

an angular divergence of about 0.01 arcsec were produced by using only one collimator crystal. Good performance of the topography system was confirmed through the observation of oscillatory rocking-curve profiles and topographic images of dislocations, growth striations and grown-in microdefects. Because of the simple optics and use of relatively high-energy X-rays, it becomes easy to carry out a stable plane-wave topographic study of Si wafers with usual thickness.

The authors thank Dr T. Shimura of Osaka University, Professor J. Matsui of Himeji Institute of Technology, Professor T. Maehama of University of the Ryukyus, Mr K. Kajiwara of JASRI, Mr S. Yamaguchi and M. Dedukuri of Toyama University for their assistance in the experiments. This work was carried out according to the SPring-8 proposal numbers 2000A0103-ND-np, 2000B0277-NM-np and 2001A0096-ND-np. Technical support by Drs Y. Suzuki, K. Umetani and K. Uesugi at SPring-8 is also appreciated.

References

Chikaura, Y., Iida, S., Kawado, S., Mizuno, K., Kimura, S., Matsui, J., Umeno, M., Ozaki, T., Shimura, T., Suzuki, Y., Izumi, K., Kawasaki, K., Kajiwara, K. & Ishikawa, T. (2001). *J. Phys. D*, **34**, A158–A162.
Chikaura, Y., Imai, M., Suzuki, Y. & Yatsurugi, Y. (1990). *J. Cryst. Growth*, **103**, 141–149.

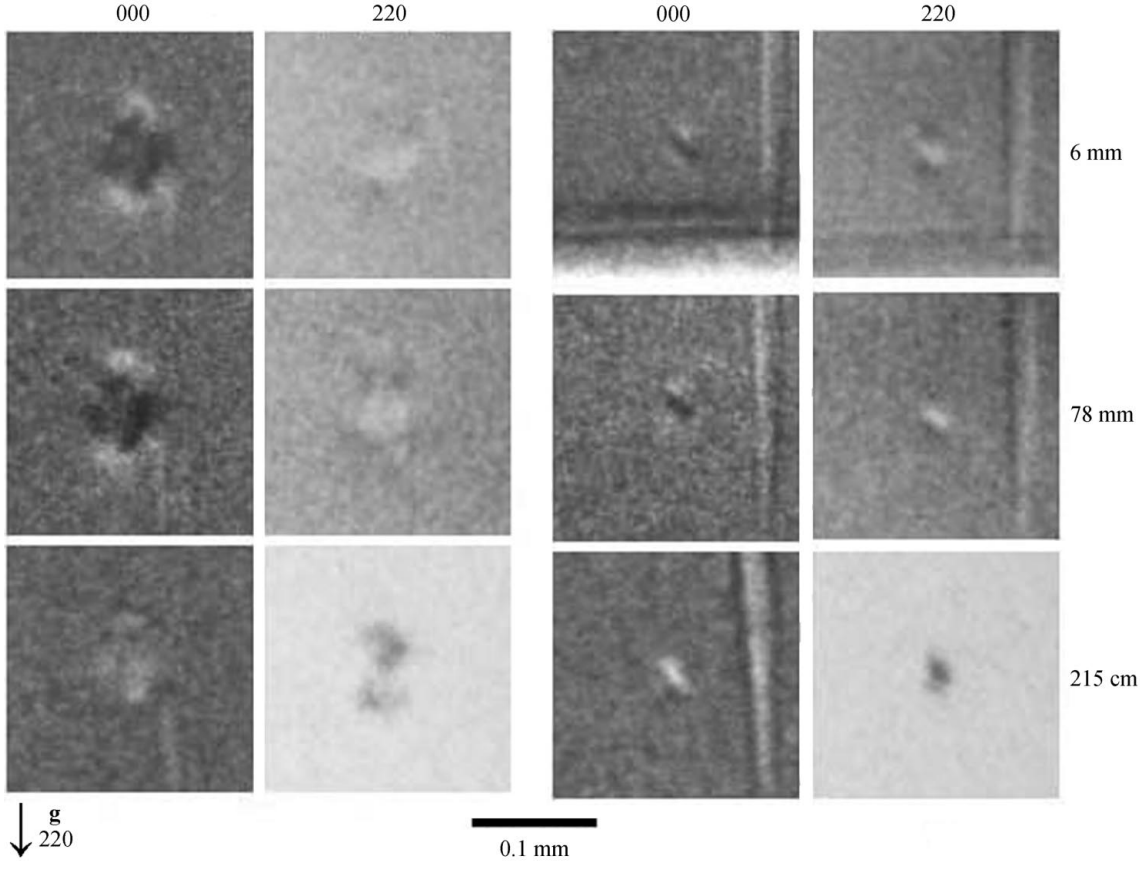

Figure 8
Comparison of topographic images of grown-in microdefects in the slowly grown CZ-Si wafer. The topographs were taken at 6 mm, 78 mm and 215 cm from the sample using 000 and 220 reflections.

Goto, S., Takeshita, K., Suzuki, Y., Ohashi, H., Asano, Y., Kimura, H., Mastushita, T., Yagi, N., Isshiki, M., Yamazaki, H., Yoneda, Y., Umetani, K. & Ishikawa, T. (2001). *Nucl. Instrum. Methods A*, **467**/**468**, 682–685.
Iida, S., Aoki, Y., Sugita, Y., Abe, T. & Kawata, H. (2000). *Jpn. J. Appl. Phys.* **39**, 6130–6135.
Ishikawa, T. (1989). *Rev. Sci. Instrum.* **60**, 2490–2493.
Kawado, S., Kojima, S., Kato, Y., Hayashi, H. & Ishikawa, T. (1990). *Defect Control in Semiconductors*, pp. 175–180. Amsterdam: Elsevier.
Kimura, S., Ishikawa, T. & Matsui, J. (1994). *Philos. Mag. A*, **69**, 1179–1187.
Kimura, S., Ishikawa, T., Mizuki, J. & Matsui, J. (1992). *J. Cryst. Growth*, **116**, 22–26.
Kimura, S., Ishikawa, T. & Matsui, J. (1996). *Defect Diffus. Forum*, **138**/**139**, 49–62.
Kudo, Y., Liu, K.-Y., Kojima, S., Kawado, S. & Ishikawa, T. (1997). *J. Electrochem. Soc.* **144**, 4035–4041.
Nango, N., Iida, S. & Ogawa, T. (1999). *J. Appl. Phys.* **86**, 6000–6004.
Sadamitsu, S., Umeno, S., Koike, Y., Hourai, M., Sumita, S. & Shigematsu, T. (1993). *Jpn. J. Appl. Phys.* **32**, 3675–3681.
Suzuki, Y., Chikaura, Y., Imai, M. & Ishikawa, T. (1993). *Jpn. J. Appl. Phys.* **32**, L958–L961.
Takeno, T., Ushio, S. & Takenaka, T. (1992). *Proceedings of the MRS Spring Meeting*, Boston, USA, 1992. Symposium E1.6.

 Received 7 November 2001 • Accepted 5 March 2002